

Efficient and Interpretable Traffic Destination Prediction using Explainable Boosting Machines

Yasin Yousif

*Department of Informatics
Clausthal University of Technology
Clausthal-Zellerfeld, Germany*

YY33@TU-CLAUSTHAL.DE

Jörg P. Müller

*Department of Informatics
Clausthal University of Technology
Clausthal-Zellerfeld, Germany*

JPM@TU-CLAUSTHAL.DE

Abstract

Developing accurate models for traffic trajectory predictions is crucial for achieving fully autonomous driving. Various deep neural network models have been employed to address this challenge, but their black-box nature hinders transparency and debugging capabilities in a deployed system. Glass-box models offer a solution by providing full interpretability through methods like Generalized Additive Models (GAM). In this study, we evaluate an efficient additive model called Explainable Boosting Machines (EBM) for traffic prediction on three popular mixed traffic datasets: Stanford drone dataset (SDD), Intersection Drone Dataset (InD), and Argoverse. Our results show that the EBM models perform competitively in predicting pedestrian destinations within SDD and InD while providing modest predictions for vehicle-dominant Argoverse dataset. Additionally, our transparent trained models allow us to analyse feature importance and interactions, as well as provide qualitative examples of predictions explanation. The full training code will be made public upon publication.

Keywords: Glass-box model, Traffic trajectory prediction, Partial dependence graphs

1 Introduction

Traffic trajectory prediction is the problem of predicting the future path of a traffic entity for a specific time horizon based on its current state, and it has been widely studied in public traffic benchmarks. Many previous works Bertugli et al. (2021); Cheng et al. (2021); Chiara et al. (2022) have been evaluated on these benchmarks under standard conditions to assess their prediction accuracy. By accurately predicting traffic trajectories, we can anticipate and avoid accidents or unsafe situations on the road, which is particularly useful for self-driving cars navigating safely.

Early methods to address this problem relied on rule-based approaches that applied general rules to determine future movements, such as social force models Helbing and Molnar (1995) or cellular automata models Maerivoet and De Moor (2005). However, these methods lack the ability to extract data-based patterns from traffic data. Later, deep learning-based models emerged Alahi et al. (2016); Gupta et al. (2018), which automatically extracted rules from the datasets and outperformed other methodologies on well-known traffic benchmarks such as Argo Chang et al. (2019) and InD Bock et al. (2020).

In recent years, some deep learning models Sadeghian et al. (2019); Yue et al. (2022); Bansal et al. (2018) have focused on enhancing the explainability of their models in a post-hoc manner. This is because a black-box model that provide accurate predictions using hidden processes for feature extraction and prediction inference can decrease trust in the model and make debugging any errors difficult.

This motivated works like Sadeghian et al. (2019); Bansal et al. (2018) to extract attention maps of the input images or works like Yue et al. (2022) to use a more interpretable input features. However, these remain partial solutions, as they still considered an approximation of the true features importance Lou et al. (2012).

An alternative approach is to use glass-box models such as linear regression, decision trees, or GAM Hastie (2017) that provide transparent explanations at the cost of lower predictive ability. Among these methods, GAM has been found to offer the best predictive results in some applications (e.g., Caruana et al. (2015); Lou et al. (2012)). Recent variants of GAM, such as Neural Additive Models (NAM) or boosted trees (EBM Nori et al. (2019)), have also shown competitive prediction results while maintaining transparency. In this work, we use an EBM model to predict traffic trajectories and evaluate our results on three well-known datasets in the field. We also extract feature importance values and partial dependence graphs that provide a clear description of how the model arrives at its predictions. These graphs show each input feature’s contribution to the output variable, offering an exact representation of the model’s decision-making process

In GAM, multiple sub-models are used, with each accessing one or two input features. These sub-models were previously shown to perform competitively when implemented using boosted trees, known as EBM. The implementation of EBM in this work is based on the Interpretml Python library Nori et al. (2019). However, there are limitations to GAM’s current formulation such as the inability to process images as input since they need to be processed collectively for useful information extraction. Additionally, having only a single output for the GAM model is another restriction that can be addressed by using full models for each output variable to predict. This approach involves having two models for each (x, y) coordinate of the predicted trajectory in this work.

Due to the difficulty in predicting a single deterministic possible output trajectory (known as mode), prediction is done for multiple modes with one EBM for each. The clustering and separation of these modes is an independent problem, addressed here by clustering the target variables

This work has two main contributions: 1) The evaluation of EBM as a glass-box model for the first time by using it as a traffic destination prediction model on three popular traffic datasets, namely SDD, InD, and Argoverse. This provides insight into how transparent and interpretable models like EBM can perform in real-world datasets. 2) We calculate partial dependence graphs and feature importance for all input features with respect to the output variable. These results offer insights into the interaction of features and their significance for traffic prediction, as well as show some selected examples of local explanations. The following sections outline GAM formula, the methodology containing the preprocessing steps, experimental evaluation, and finally, the conclusions.

2 GAM Formula

To define GAM and GA2M mathematical formulas, let $\mathcal{D} = (\mathbf{x}_i, y_i)_1^N$ be the training dataset, and $\mathbf{x}_i = (x_{i1}, x_{i2}, \dots, x_{ip})$ the input vector for the target variable of y_i , and x_j is the feature j value. Therefore GA2M, Caruana et al. (2015), will try to fit the dataset as the following expression:

$$g(E[y]) = \beta_0 + \sum_j f_j(x_j) + \sum_{k \neq j} f_{kj}(x_k, x_j) \quad (1)$$

Where f_j is the model mapping function for feature j , f_{kj} is for the interaction between features (j, k) , g is the link function and β_0 is the bias parameter. This model will be completely explainable, because one can draw the exact relationship between the input feature x_j and the target y as 2D plot or as heatmap for the interaction between two features as in the last term.

With EBM, in addition to fitting each feature alone, a fast search for the most useful feature interactions in the dataset is done as in Lou et al. (2013), then the top k features interactions are used in the model, where k is selected using cross validation.

List of the hyperparameters of EBM in this work are provided in appendix B.

3 Methodology

In our approach, we generate multiple outputs representing different modes and assign probabilities for each mode. We detail the representation of multi-modality and probability calculation in the first two subsections. Following that is three subsections to focus on input and output shape specifications for SDD, InD, and Argo datasets, respectively.

3.1 Multiple Modes Output

Most traffic prediction benchmarks require predicting multiple possible future trajectories with a probability distribution over them, which is known as multi-modal output Phan-Minh et al. (2020). This condition ease the prediction task; however, in our case, EBM has a unimodal output, so we can train separate models for each mode to obtain multi-modal output.

However, defining these modes is another challenge. Many approaches were used in the literature, like using a set of rule-based modes Phan-Minh et al. (2020), or with an implied clustering in multiple branches output Yousif and Müller (2022). In this work, we manually cluster the target points using either K-means clustering algorithm for SDD and InD datasets (see figure 1) or uniform splitting over x-axis followed by y-axis to equally distribute samples across modes for Argo dataset (see figure 2).

3.2 Outputs Probabilities

Each of the previous outputs should be assigned a probability normalized over all the outputs. This will add flexibility to the prediction because it can give an arbitrary number of outputs and then only the most probable K output will be taken. In this work, probability estimation of modes is done by finding the sum of the loglikelihood of each of the mode-level

models \mathcal{L}_1 with the corresponding loglikelihood of its predictions under the distribution of the main uni-modal model \mathcal{L}_2 , as in equation (2).

$$\mathcal{L}_{mode_x} = \lambda_1 \mathcal{L}_1(\pi_{mode_x}(x), \sigma_{mode_x}) + \lambda_2 \mathcal{L}_2(\pi_{mode_x}(x), \sigma_{all_x}) \quad (2)$$

After finding that for both of x and y axes, we take a weighted sum of them for each mode in equation (3). Finally, the top 20 probable output will be taken as final.

$$\mathcal{L}_{mode} = \lambda_3 \mathcal{L}_{mode_x} + \lambda_4 \mathcal{L}_{mode_y} \quad (3)$$

The weights λ_3 and λ_4 are determined based on relative standard deviation between axes, while λ_1 and λ_2 can be experimentally set

3.3 SDD

In the SDD experiments, our models predict the final point of each trajectory, which the most challenging part to predict. This allows for comparison with other methods in the SDD benchmark using the Final Displacement Error (FDE) metric. In this work, we use pixels as the standard unit of measurement, similar to previous works such as Phan-Minh et al. (2020); Chiara et al. (2022); Deo and Trivedi (2020).

After loading data files from 60 scenes, they will be split according to a common splitting standards as in Deo and Trivedi (2020), where only pedestrians' trajectories are considered. The training and validation sets are combined and passed to the fitting function.

The input features of our model include the last 7 positions relative to the 8th position, with a timestep of 400 ms between each two positions. These points are rotated by the latest heading angle, and we also consider the sum of lost, occluded, and generated flags for the eight input points. Finally, the width and height of the object at the 8th point are included as well.

The target variables consist of the (x, y) coordinates of the object after 4.8 seconds, rotated and transferred in a manner similar to the input trajectory case. This requires two EBM models for each coordinate.

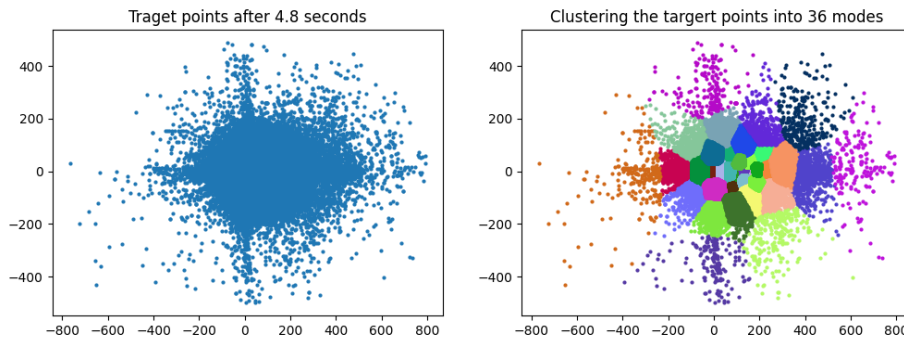


Figure 1: Left: full training set of target variable. Right: target variable set is split into multiple clusters.

Figure 1 on the left shows the target variable for both training and validation sets of pedestrians combined. The data is concentrated towards the centre, but there are some

points that are far away due to noise in SDD as mentioned earlier (Becker et al. (2018)). To address this issue, we removed any point outside a specific range for both x and y , which represents only 0.005% of the total data.

In previous works like Mangalam et al. (2021); Guo et al. (2022); Deo and Trivedi (2020), evaluations typically involved using 20 modes as outputs. However, since we started by clustering the data into 36 groups using k-means algorithm (as shown in figure 1 on the right), and then trained two separate models for each x and y within these clusters, only the most probable 20 pairs of predictions will be selected. Furthermore, we also trained global uni-modal models to help identify the best models later in the process.

3.4 InD

For each scene, the data from its CSV file is read, and then we formulate the input similarly to SDD, as in previous studies such as Bertugli et al. (2021); Chiara et al. (2022). This includes the last 8 positions of the past 3.2 seconds, which consist of their position, velocity, acceleration, heading, width, and height. The target variable is the traffic entity’s position after 4.8 seconds; however, only pedestrian predictions are considered in this case. Similar to SDD, we split the target variable data into 50 modes.

3.5 Argoverse

3.5.1 PREPROCESSING STEPS

For Argoverse Chang et al. (2019), we aim to represent all available input data, including the road network and other nearby traffic entities. However, before feeding this information into our EBM model, some preprocessing is required to make it easier for the model while also maintaining interpretability of the features.

We then split the dataset based on the type of ego traffic entity present in each scene. This results in different sets of models being trained for various types of entities (cars, bicycles, buses, pedestrians, and motorcyclists), with approximately 88% of the data representing cars while the rest is distributed among these other categories.

3.5.2 ROAD NETWORK DATA

The road network is initially represented as a binary image, where the drivable area has high value. Next, different sub-areas representing various modes are created based on the target variable (shown in figure 2). These mask parts of the drivable area and find the geometric centre of each mode rectangle. However, a tuple of zeros will be returned if there is no drivable area available.

Using these same sub-area modes from figure 2 is an appropriate choice because they represent the most relevant part of the road for its corresponding prediction. Finally, the point of collision (POC) based on Post encroachment time (PET) (Nasernejad et al. (2023)) is included as input features to capture traffic movement in the area. A detailed explanation of this calculation can be found in appendix A.

3.5.3 DEFINING MODES

Similar to SDD and InD, we rotate all points and move them to the last input directions and positions for of their respective trajectory. For the challenge conditions, 5 seconds of trajectory history are required as input, while a prediction is made for 6 seconds into the

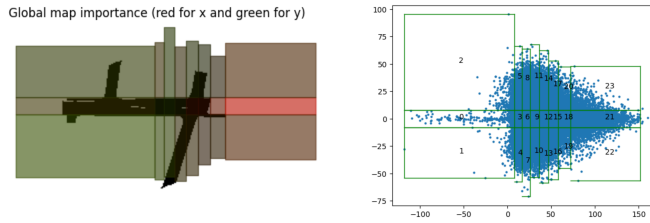


Figure 2: How the road network is represented (Left). Each mode rectangle (Right) return the geometric center of the drivable area underneath it. Red and green colors represent importance for x and y respectively

future. To achieve this, we define 24 modes on the target variable (shown in figure 2 for vehicles) by splitting uniformly along the x-axis and manually dividing along the y-axis to create large central modes. Probabilities are calculated similarly to SDD and InD, with the top 6 mode predictions being selected as final.

4 Experimental Evaluation

After training all models, we evaluate their performance using final displacement errors displayed in table 1. The additive models show competitive results on SDD and are comparable to state-of-the-art (SoTA) on InD without road map input. However, they do not perform as well on Argoverse. One factor for that is that cars predication is a harder problem than pedestrians’ predication and rely heavily on nearby elements and roadmap.

Table 1: Minimum final displacement errors for 20 modes on SDD and InD, and for 6 modes on Argoverse for EBM (ours) and a subset of SoTA previous methods

Dataset	EBM	SEPT	ST-GAT	AC-VRNN	S-GAN	Y-Net	GOAL-SAR	P2T	PEC	TDOR
SDD (pixels)	14.70	-	-	-	41.44	11.85	11.83	14.08	15.88	10.46
InD	0.54	-	1	0.80	0.99	0.56	0.54	-	-	-
Argoverse*	3.88	1.09	-	-	-	-	-	-	-	-

*Cars only predication. Updated leaderboard here

SEPT: Lan et al. (2023), ST-GAT: Huang et al. (2019),AC-VRNN: Bertugli et al. (2021)

S-GAN: Gupta et al. (2018),Y-Net: Mangalam et al. (2021),GOAL-SAR: Chiara et al. (2022)

P2T: Deo and Trivedi (2020),PEC: Mangalam et al. (2020),TDOR: Guo et al. (2022)

Figures 3 to 8 show global feature importance bars for each dataset using unimodal models. Additionally, partial dependence graphs of the six most important features on (x and y) are shown. It is noted in general that the last steps are the most influencing input in all of the datasets. Another interesting remark is that the acceleration is very crucial in InD dataset models. Examples of local explanations can be found in appendix C.

5 Conclusion

In this comprehensive analysis of generalized additive models for traffic prediction, we have seen their notable performance when it comes to predicting pedestrian movements. In fact, they outperform state-of-the-art deep learning models in terms of accuracy. Furthermore, as

TRAFFIC DESTINATIONS PREDICTION WITH GAMs

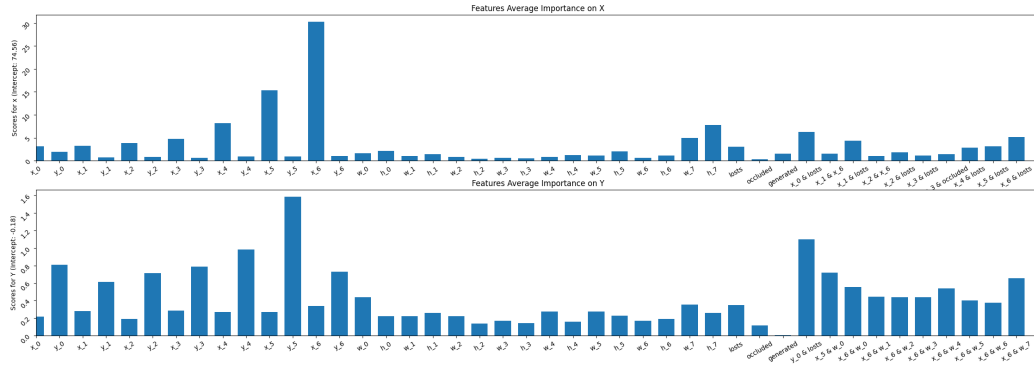


Figure 3: SDD: Global Feature Average Importance for X and Y

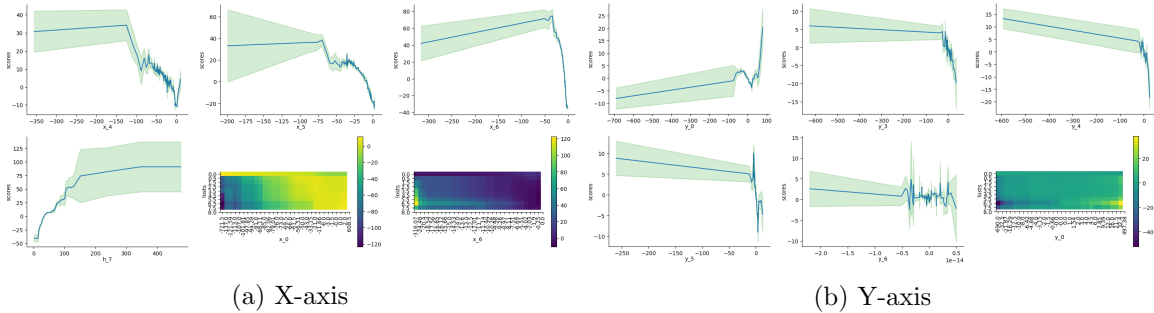


Figure 4: SDD: Partial Dependence Graph on X and Y axis for the best 6 features

a glass-box model, they offer full transparency and interpretability. However, one potential drawback is their limited ability to predict multiple variables per model, which requires the training of numerous individual models for each point along the trajectory. Future research will focus on developing more effective image processing techniques for the road network, allowing us to fully leverage the environmental information available in the data.

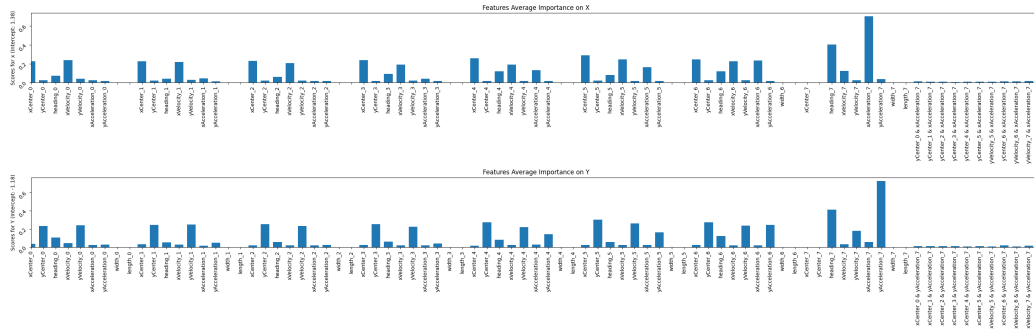


Figure 5: InD: Global Feature Average Importance for X and Y

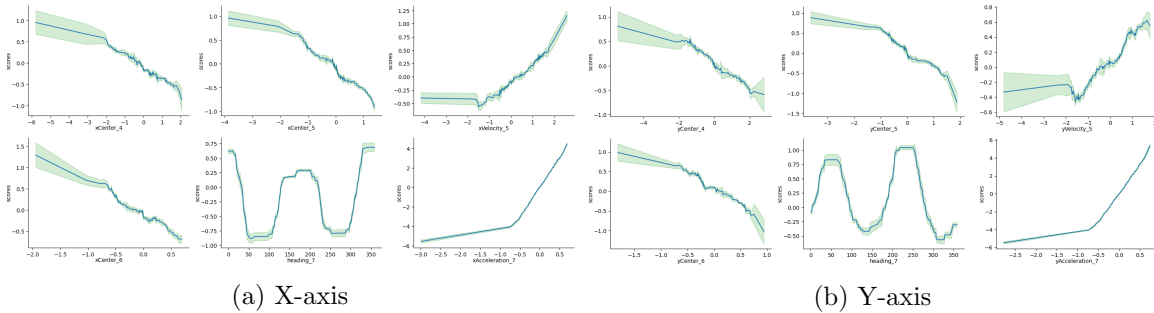


Figure 6: InD: Partial Dependence Graph on X and Y axes for the best 6 features

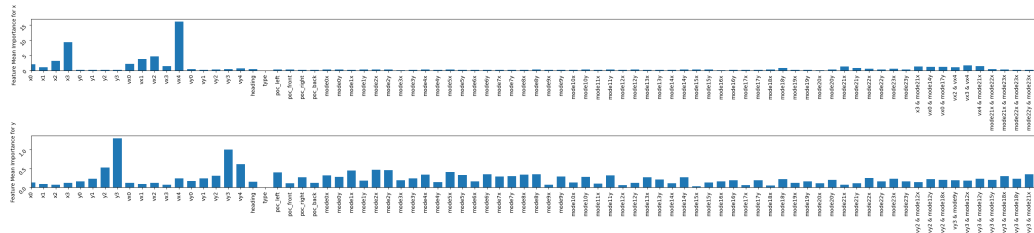


Figure 7: Argo: Global Feature Average Importance for X and Y

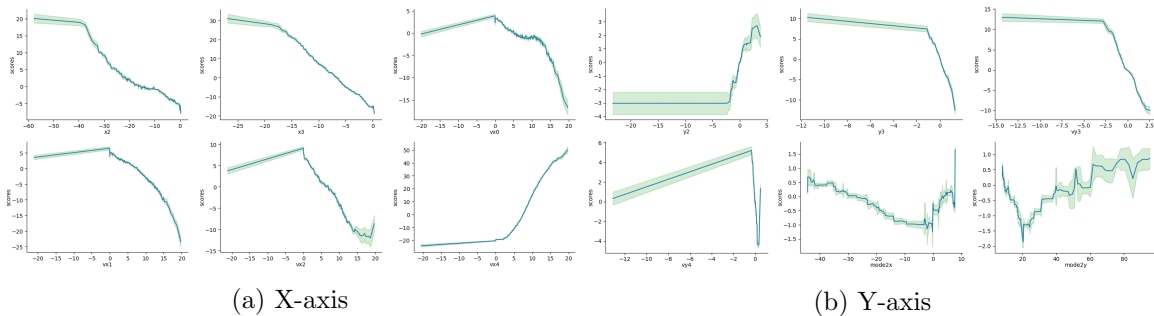


Figure 8: Argo: Partial Dependence Graph on X and Y axis for the best 6 features

Reproducibility Statement and Supplementary Material

The full training code is split into three notebooks for the three datasets, with the instruction of how to run them here:

<https://anonymous.4open.science/r/GAM4Traffic-5785/Readme.md>

The full training (and testing) can be reproduced fairly fast on modest hardware. In our case, the training was done on (Intel(R) Core(TM) i7-10850H CPU)

References

- A. Alahi, K. Goel, V. Ramanathan, A. Robicquet, L. Fei-Fei, and S. Savarese. Social lstm: Human trajectory prediction in crowded spaces. In *Proceedings of the IEEE conference on computer vision and pattern recognition*, pages 961–971, 2016.
- M. Bansal, A. Krizhevsky, and A. Ogale. Chauffeurnet: Learning to drive by imitating the best and synthesizing the worst. *arXiv preprint arXiv:1812.03079*, 2018.
- S. Becker, R. Hug, W. Hübner, and M. Arens. An evaluation of trajectory prediction approaches and notes on the trajnet benchmark. *arXiv preprint arXiv:1805.07663*, 2018.
- A. Bertugli, S. Calderara, P. Coscia, L. Ballan, and R. Cucchiara. Ac-vrnn: Attentive conditional-vrnn for multi-future trajectory prediction. *Computer Vision and Image Understanding*, 210:103245, 2021.
- J. Bock, R. Krajewski, T. Moers, S. Runde, L. Vater, and L. Eckstein. The ind dataset: A drone dataset of naturalistic road user trajectories at german intersections. In *2020 IEEE Intelligent Vehicles Symposium (IV)*, pages 1929–1934. IEEE, 2020.
- R. Caruana, Y. Lou, J. Gehrke, P. Koch, M. Sturm, and N. Elhadad. Intelligible models for healthcare: Predicting pneumonia risk and hospital 30-day readmission. In *Proceedings of the 21th ACM SIGKDD international conference on knowledge discovery and data mining*, pages 1721–1730, 2015.
- M.-F. Chang, J. Lambert, P. Sangkloy, J. Singh, S. Bak, A. Hartnett, D. Wang, P. Carr, S. Lucey, D. Ramanan, et al. Argoverse: 3d tracking and forecasting with rich maps. In *Proceedings of the IEEE/CVF conference on computer vision and pattern recognition*, pages 8748–8757, 2019.
- H. Cheng, W. Liao, M. Y. Yang, B. Rosenhahn, and M. Sester. Amenet: Attentive maps encoder network for trajectory prediction. *ISPRS Journal of Photogrammetry and Remote Sensing*, 172:253–266, 2021.
- L. F. Chiara, P. Coscia, S. Das, S. Calderara, R. Cucchiara, and L. Ballan. Goal-driven self-attentive recurrent networks for trajectory prediction. In *Proceedings of the IEEE/CVF Conference on Computer Vision and Pattern Recognition*, pages 2518–2527, 2022.
- N. Deo and M. M. Trivedi. Trajectory forecasts in unknown environments conditioned on grid-based plans. *arXiv preprint arXiv:2001.00735*, 2020.

- K. Guo, W. Liu, and J. Pan. End-to-end trajectory distribution prediction based on occupancy grid maps. In *Proceedings of the IEEE/CVF Conference on Computer Vision and Pattern Recognition*, pages 2242–2251, 2022.
- A. Gupta, J. Johnson, L. Fei-Fei, S. Savarese, and A. Alahi. Social gan: Socially acceptable trajectories with generative adversarial networks. In *Proceedings of the IEEE conference on computer vision and pattern recognition*, pages 2255–2264, 2018.
- T. J. Hastie. Generalized additive models. In *Statistical models in S*, pages 249–307. Routledge, 2017.
- D. Helbing and P. Molnar. Social force model for pedestrian dynamics. *Physical review E*, 51(5):4282, 1995.
- Y. Huang, H. Bi, Z. Li, T. Mao, and Z. Wang. Stgat: Modeling spatial-temporal interactions for human trajectory prediction. In *Proceedings of the IEEE/CVF international conference on computer vision*, pages 6272–6281, 2019.
- Z. Lan, Y. Jiang, Y. Mu, C. Chen, S. E. Li, H. Zhao, and K. Li. Sept: Towards efficient scene representation learning for motion prediction. *arXiv preprint arXiv:2309.15289*, 2023.
- Y. Lou, R. Caruana, and J. Gehrke. Intelligible models for classification and regression. In *Proceedings of the 18th ACM SIGKDD international conference on Knowledge discovery and data mining*, pages 150–158, 2012.
- Y. Lou, R. Caruana, J. Gehrke, and G. Hooker. Accurate intelligible models with pairwise interactions. In *Proceedings of the 19th ACM SIGKDD international conference on Knowledge discovery and data mining*, pages 623–631, 2013.
- S. Maerivoet and B. De Moor. Cellular automata models of road traffic. *Physics reports*, 419(1):1–64, 2005.
- K. Mangalam, H. Girase, S. Agarwal, K.-H. Lee, E. Adeli, J. Malik, and A. Gaidon. It is not the journey but the destination: Endpoint conditioned trajectory prediction. In *Computer Vision—ECCV 2020: 16th European Conference, Glasgow, UK, August 23–28, 2020, Proceedings, Part II 16*, pages 759–776. Springer, 2020.
- K. Mangalam, Y. An, H. Girase, and J. Malik. From goals, waypoints & paths to long term human trajectory forecasting. In *Proceedings of the IEEE/CVF International Conference on Computer Vision*, pages 15233–15242, 2021.
- P. Nasernejad, T. Sayed, and R. Alsaleh. Multiagent modeling of pedestrian-vehicle conflicts using adversarial inverse reinforcement learning. *Transportmetrica A: transport science*, 19(3):2061081, 2023.
- H. Nori, S. Jenkins, P. Koch, and R. Caruana. Interpretml: A unified framework for machine learning interpretability. *arXiv preprint arXiv:1909.09223*, 2019.

- T. Phan-Minh, E. C. Grigore, F. A. Boulton, O. Beijbom, and E. M. Wolff. Covernet: Multimodal behavior prediction using trajectory sets. In *Proceedings of the IEEE/CVF conference on computer vision and pattern recognition*, pages 14074–14083, 2020.
- A. Sadeghian, V. Kosaraju, A. Sadeghian, N. Hirose, H. Rezatofighi, and S. Savarese. Sophie: An attentive gan for predicting paths compliant to social and physical constraints. In *Proceedings of the IEEE/CVF conference on computer vision and pattern recognition*, pages 1349–1358, 2019.
- Y. M. Yousif and J. P. Müller. Generating explanatory saliency maps for mixed traffic flow using a behaviour cloning model. In *International Workshop on Multi-Agent Systems and Agent-Based Simulation*, pages 107–120. Springer, 2022.
- J. Yue, D. Manocha, and H. Wang. Human trajectory prediction via neural social physics. In *European Conference on Computer Vision*, pages 376–394. Springer, 2022.

Appendix A. Representing Nearby Traffic

The future trajectory is also influenced by nearby entities, which need to be compressed for better training and model interpretability. One approach to achieve this is through direct measures related to movement such as Time to collision (TTC) or Post encroachment alignment (PET). However, both of these methods rely on time values while we require position predictions. Therefore, in this section, the point of collision (POC) will be used as a measure. POC assumes that two objects have constant velocity movement and predicts their expected point of collision. To account for all possible scenarios, four different directions of movement are assumed for the ego object, as shown in figure 9. The mean of other objects’ POC with those directions is calculated to give one point per direction. If no point is found for a particular direction, a default mid-point will be returned.

Lastly, it should be noted that since one coordinate is redundant given the movement direction; only four values representing the x coordinates of these four points are taken as input features.

Appendix B. EBM Hyperparameters

List of the hyperparameters of EBM in this work are shown in table 2, such as maximum number of leafs, and maximum training round, learning rate, maximum feature bins, and outer bags.

Appendix C. Qualitative Examples of Local Explanation

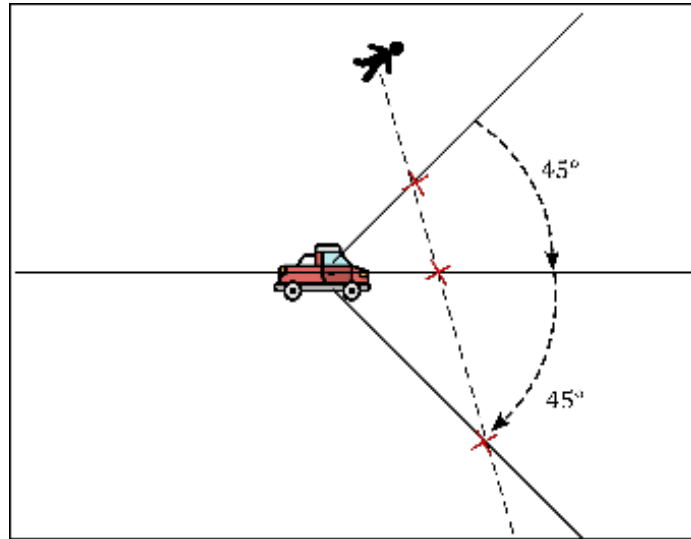


Figure 9: Finding the points of collision for four directions

Table 2: EBM Hyperparameters

Hyperparameter	Value
Maximum feature bins	256
Maximum interaction bins	32
Maximum training rounds	5000
Learning rate	0.01
Maximum number of leaf	3
Outer bags	8
Validation size	15%

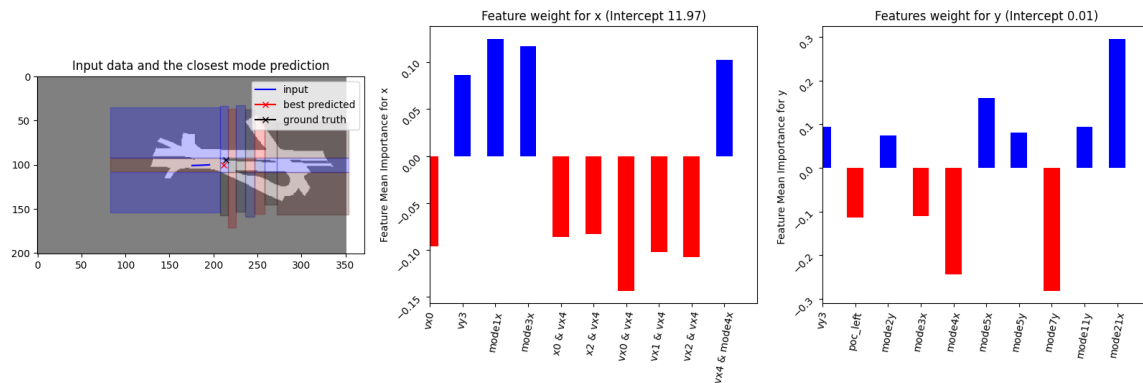


Figure 10: Argo: Local Example of the best mode in one case. Road highlighted according to X values (red increase it and blue decrease it)

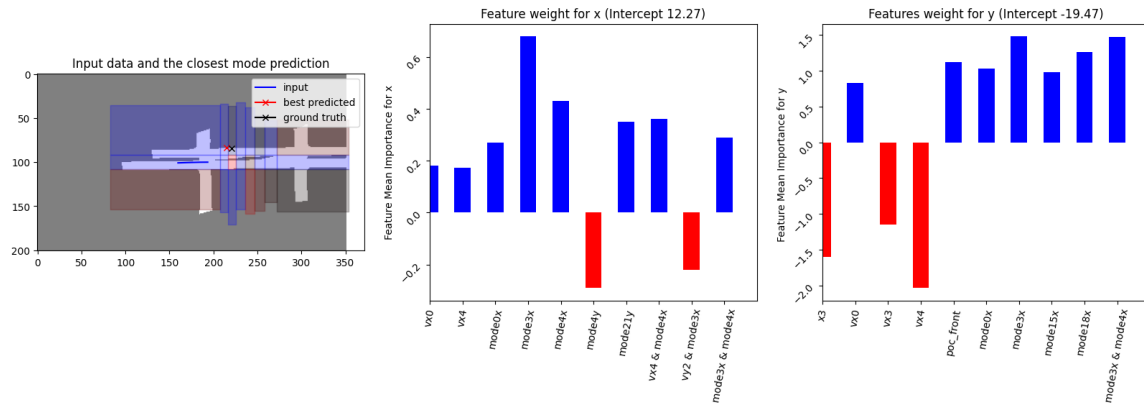


Figure 11: Argo: Local Example of the best mode in one case. Road highlighted according to X values (red increase it and blue decrease it)

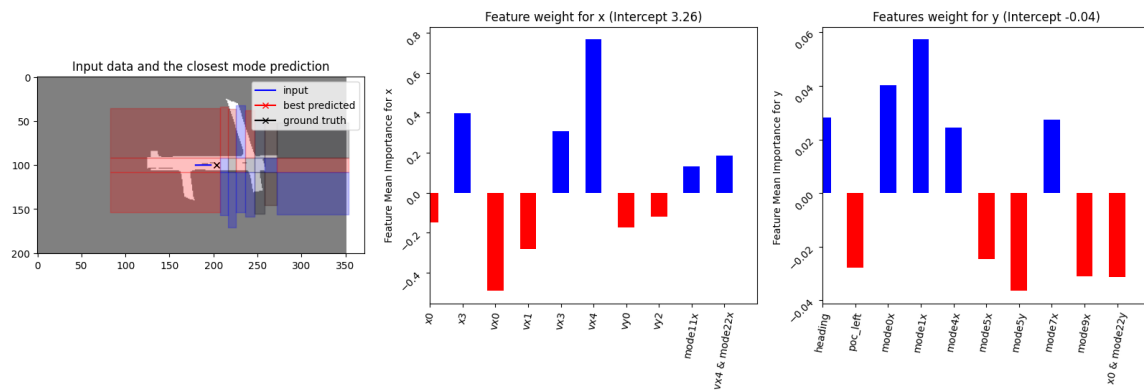


Figure 12: Argo: Local Example of the best mode in one case. Road highlighted according to X values (red increase it and blue decrease it)

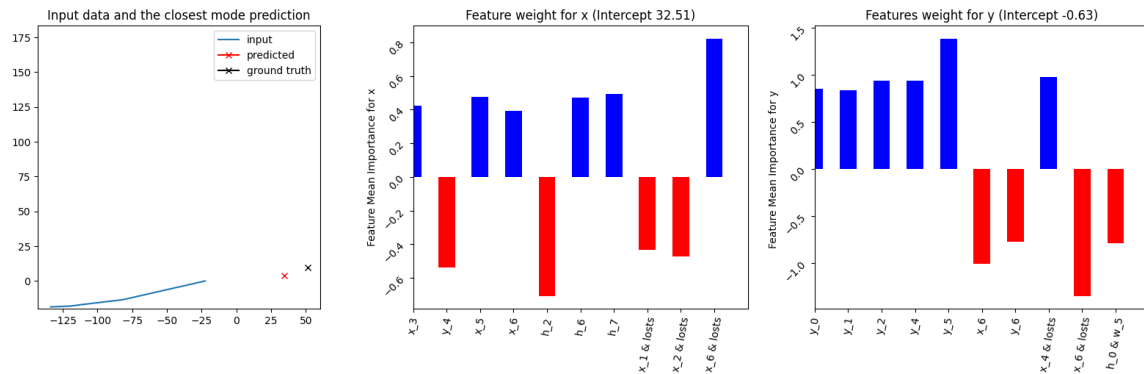


Figure 13: SDD: Local Example for one point prediction

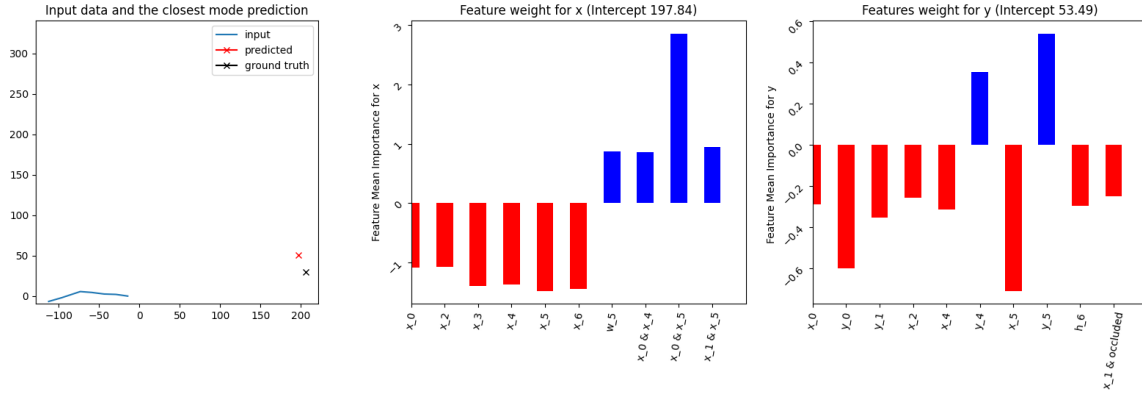


Figure 14: SDD: Local Example for one point prediction

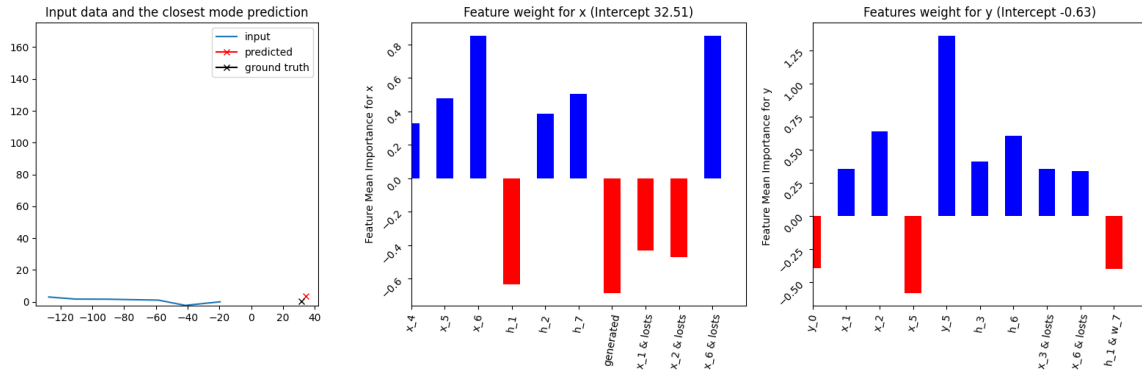


Figure 15: SDD: Local Example for one point prediction

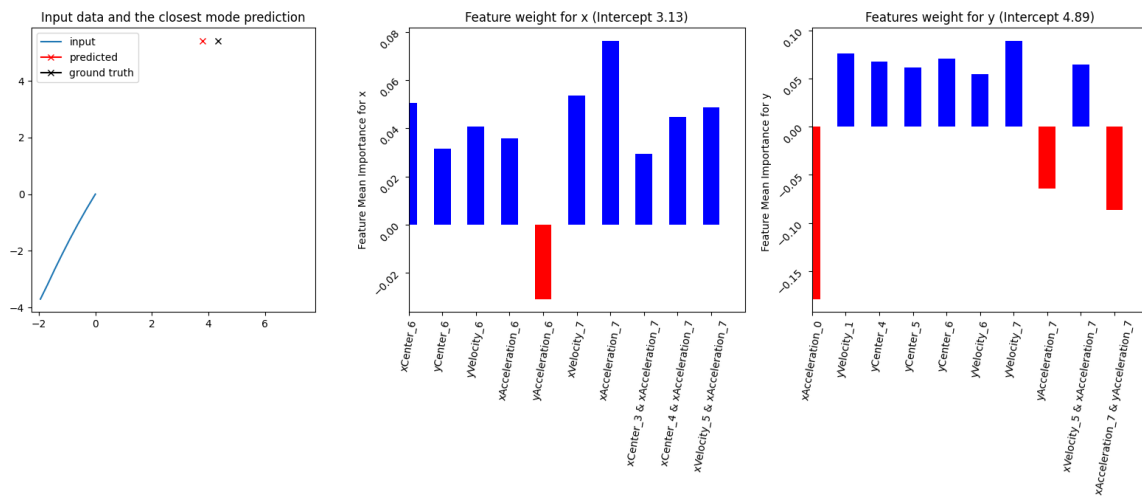


Figure 16: InD: Local Example for one point prediction